Macromolecules

ARTICLE

pubs.acs.org/Macromolecules

Structure of Ultralong Polyaniline Nanofibers Using Initiators

Zoran D. Zujovic,*[,†] Yue Wang,[‡] Graham A. Bowmaker,[†] and Richard B. Kaner[‡]

[†]Department of Chemistry, Polymer Electronic Research Centre, The University of Auckland, Private Bag 92019, Auckland, New Zealand

[‡]Department of Chemistry and Biochemistry and California NanoSystems Institute, University of California, Los Angeles, Los Angeles, California 90095, United States

ABSTRACT: Detailed morphological and structural characterization of high-aspect-ratio polyaniline nanofibers obtained using a small amount of *p*-aminodiphenylamine (dimer) or *p*-phenylenediamine (diamine monomer) as an initiator into a rapidly mixed reaction is presented. Structural characteristics have been investigated by FT-IR, UV−vis−NIR, solid-state ^{13}C NMR, and ^{15}N NMR, while the morphology was examined using scanning electron microscopy (SEM) and transmission electron microscopy (TEM). Nanofibers obtained with the addition of an initiator appear longer and less entangled than those obtained without any initiators. TEM analysis revealed a distinct morphological difference between the nanofibers synthesized with different additives. The *p*-aminodiphenylamine-initiated polyaniline possesses an electrical conductivity of 3.0 S cm^{-1}, while the *p*-phenylenediamine-initiated counterpart has a conductivity of 1.7 S cm^{-1}. FT-IR, $^{1}H-^{13}C$ cross-polarization (CP), ^{15}N direct polarization (DP), and UV−vis−NIR spectroscopy confirm that a regular polyaniline structure prevails in both nanofibers. Therefore, various initiators only result in a slight difference in the final polymer molecular structure and physical properties, but such minor divergence dictates the subsequent chain assembly and affects the supramolecular morphology significantly.

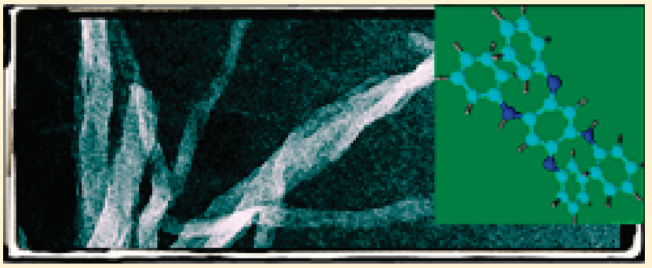

I. INTRODUCTION

Since their discovery, conducting polymers have attracted great interest due to their potential use as inexpensive and flexible organic (semi)conducting layers in various applications such as electronics, photovoltaic devices, and supercapacitors.[1] In recent years, studies toward the formation of one-dimensional (1-D) nanostructures such as fibers, wires, rods, and tubes of conducting polymers have flourished because of the proven advantages of such materials in many applications that lead to superior performance characteristics compared to those of their currently used bulk counterparts.[2−12] Among all the conducting polymers, polyaniline (PANI) nanofibers are one of the most intensively studied systems because of their remarkable propensity to form anisotropic structures and also the unique, simple acid−base doping−dedoping chemistry.[13] Synthetic routes toward PANI nanofibers include template-guided methods such as those using zeolites,[14,15] surfactants or bulky dopant acids,[16−19] nanowire seeding,[20] and biotemplates.[21] A number of techniques have also been developed to synthesize PANI nanofibers without any external templates such as interfacial polymerization,[22,23] rapidly mixed polymerization,[24] dilute polymerization,[25,26] sonochemical,[27] and radiolytic-assisted synthesis.[28] Despite the simplicity of these procedures, the formation mechanisms involved in such processes are quite complex. Although a number of theories have been proposed to describe these processes,[29,30] considerable work remains to be done to achieve a better understanding.

We recently discovered that the introduction of a small amount of *p*-aminodiphenylamine (dimer) or *p*-phenylenediamine (monomer) into a rapidly mixed reaction greatly improves the quality of the PANI nanofibers.[30] Conventional PANI nanofibers synthesized without such additives are typically only up to 1 μm in length. However, when an additive is incorporated, the nanofibers produced become ultralong as on average their length ranges from several micrometers up to ∼10 μm.[30] Such an enhancement in aspect ratio could potentially facilitate better postsynthetic alignment and be advantageous in single fiber device fabrication and measurement, which is crucial for realizing the practical use of such materials in nano- and microelectronics. Mechanistic studies of these PANI nanofibers reveal that the additive serves as homogeneous nucleation centers that accelerate the reaction rate and promote the formation of high-aspect-ratio nanofibers. They remain in the final polymer chain without changing the typical PANI chain structure markedly. Therefore, the additive is considered an initiator for the polymerization and the succeeding supramolecular assembly.[30] However, current studies of PANI nanosturctures are mostly limited to morphological observations with SEM and characterization techniques such as UV−vis spectroscopy and cyclic voltammetry (CV) for the determination of their oxidation states. Little is known about precisely how PANI nanofibers are assembled from their molecular chains. Thus, considerable work remains to be done in order to elucidate the exact mechanism at the molecular level. One

Received: December 5, 2010
Revised: March 11, 2011
Published: March 28, 2011

Scheme 1. Initiators Used in This Work

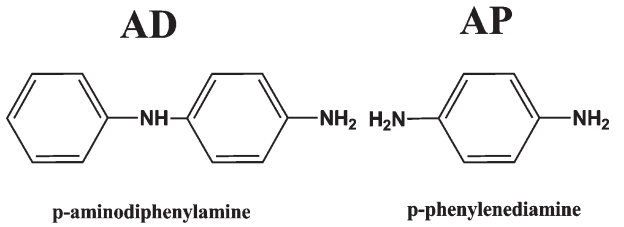

representative example for the deficiency of knowledge in this area is that it has been reported that PANI nanofibers synthesized with either aniline dimer or *p*-phenylenediamine as the initiator appear identical under SEM.[30,31] However, when they are incorporated into the same rapidly mixed reactions of aniline derivatives, the choice of initiator becomes crucial. For example, when aniline dimer is used in the polymerization of *o*-anisidine, nanofibers are obtained, whereas the analogous reaction with *p*-phenylenediamine yields only granule-shaped agglomerates that are indistinguishable from those synthesized without any initiators.[31] The effect is reversed for poly(2-chloroaniline). The precise reason behind such effects is not clear, but the distinct differences in morphology suggest that the minute amount of initiators could play a significant role in dictating the structures of PANI at both the molecular and the supramolecular level. Here, we seek to establish correlations between the structure at the chain level and that at the supramolecular level for such PANI nanofibers.

In our previous reports on standard PANI, PANI nanofibers, and self-assembled PANI nanotubes obtained with the "falling pH" technique, solid-state NMR has proven to be a useful and sensitive tool to study the different PANI nanostructures at the atomic level.[6,32−35] With the NMR information, it is possible to develop a clearer mechanistic understanding of the formation of PANI nanofibers using additives and their possible structural differences at the atomic level as well as to tune reaction conditions in order to obtain a preferred morphology. Therefore, our goal here is to explore the structures of these nanofibers using solid-state NMR and to relate these findings to other analytical data including SEM, TEM, UV−vis−NIR, FT-IR, and conductivity measurements in order to gain insights into the effects of additives on the final superstructure and the resulting structure −property relationships.

II. EXPERIMENTAL SECTION

Synthesis. The nanofibers were synthesized following a previously reported method.[22] 3−4 mg of *p*-aminodiphenylamine (aniline *p*-dimer) or *p*-phenylenediamine was dissolved in 500 μL of methanol, and the resulting solution added to a solution of 0.8 mmol of ^{15}N-labeled aniline dissolved in 10 mL of 1 M HCl. This initiator-containing monomer solution was then rapidly mixed with the oxidant solution containing 0.2 mmol of ammonium peroxydisulfate in 10 mL of 1 M HCl. The mixture was vigorously shaken for about 5 s and left undisturbed for 1 day. The crude product was purified by dialysis against deionized water for 3 days followed by dialysis against 0.1 M NH_4OH aqueous solution for another day to dedope the product. The purified product was dried in a 55 °C oven and used for solid-state NMR studies. A sample obtained from aniline polymerization initiated with *p*-aniline dimer (Scheme 1A) will be henceforth referred to as the sample AD ("AD" for aniline−dimer) as distinct from a sample obtained in polymerization initiated using *p*-phenylenediamine (see Scheme 1B) which will be referred to as the sample AP ("AP" for aniline−phenylenediamine).

Solid-State NMR spectroscopy. All solid-state NMR experiments were carried out on dry, dedoped powder of nanofibers using a Bruker AVANCE 300 spectrometer operating at 300.13 MHz proton frequency. Spectra were obtained by using the CP MAS (cross-polarization magic angle spinning) and direct polarization (DP)−Bloch decay techniques. The experiments were carried out using a 7 mm Bruker spinning probe with zirconia rotors. The magic angle was adjusted by maximizing the sidebands of the ^{79}Br signal of a KBr sample.

^{13}C CP MAS NMR Experiments. The proton 90° pulse duration was 4.2 μs, and the frequency of the decoupling field was 62.5 kHz. The contact time was 1.5 ms. The recycle delay was 1−2 s, and spectral width was 40 kHz. Standard CP experiments were carried out with 4000−5000 scans at ambient temperature using samples enclosed in the rotors. The ^{13}C chemical shift scale is referenced to TMS. Samples were rotated at 7000 Hz. Variable contact time (VCT) experiments were performed with 2000−2500 scans. The 12 variable contact time periods ranged from 30 μs up to 10 ms.

^{15}N CP and Direct Polarization (DP) MAS NMR Experiments. The parameters for "standard" ^{15}N CP, proton relaxation experiments with ^{15}N detection (T_1^H(N)), and variable contact time (VCT) measurements were as follows: all ^{15}N spectra were acquired at a spectrometer frequency of 30.41 MHz. The sample rotation frequency was 4500 Hz. ^{15}N chemical shifts were measured to external $^{15}NH_4Cl$ but are reported relative to $^{15}NH_4NO_3$ (δ $^{15}NH_4^+$ = 0 ppm). The spectral width was 30.03 kHz. The 90° pulse was 7.3 μs, and the recycle delay was 1.5−3 s. To explore the effects of T_1^H time on the quantitative proton inversion−recovery relaxation experiments, (T_1^H(N)) experiments were carried out with nitrogen detection. The recycle delay for these experiments was 50 s. The number of scans was as follows: CP: sample AD, 5000; sample AP, 10 000. VCT: sample AD, 1300; sample AP, 2500. T_1^H(N): samples AD and AP, 70. The DP experiments were carried out using the one-pulse-and-collect approach with heteronuclear decoupling during the acquisition interval. The recycle delay was determined from the experiments with different recycle delay ranging from 50 up to 500 s, until the intensities remained unchanged. The recycle delay for the final experiments was 300 s, and the spectra were obtained using 100 scans.

^{1}H MAS NMR Experiments. In order to check T_1^H time obtained with ^{15}N detection and estimate recycle delay for CP experiments, proton inversion−recovery relaxation experiments with ^{1}H detection were carried out with the following parameters: the recycle delay was 25 s, the series of 12 spectra was obtained using one scan for each experiment, and the proton 90° pulse duration was 4 μs.

Electron Microscopy. Samples for scanning electron microscopy (SEM) and transmission electron microscopy (TEM) were prepared by drop-casting an aqueous dispersion of the doped PANI nanofibers onto a silicon wafer and a TEM grid, respectively. SEM images were taken with a JEOL JSM-6700-F field emission SEM microscope, and TEM images were taken with a FEI/PHILIPS CM 120 transmission electron microscope.

FT-IR Measurements. The spectra were obtained using a Perkin-Elmer Spectrum 100 Series spectrometer (ATR mode, diamond/ZnSe crystal, at 4 cm^{-1} resolution).

UV−vis−NIR Measurements. UV−vis−NIR (near-infrared) spectra of the nanofiber dispersion in water were taken with a quartz cuvette that has a 1 mm light path length on a Shimadzu UV-3101 PC UV−vis−NIR scanning spectrophotometer.

Conductivity Measurements. Aqueous dispersions of both samples in their protonated, emeraldine salt oxidation states were drop-cast on SiO_2 substrates. Gold electrodes were sputtered on top of the films via a patterned mask. Four-point probe sheet resistances were measured and the thicknesses of the films were determined by a Dektak 6 profilometer on three separate samples. Film conductivities of

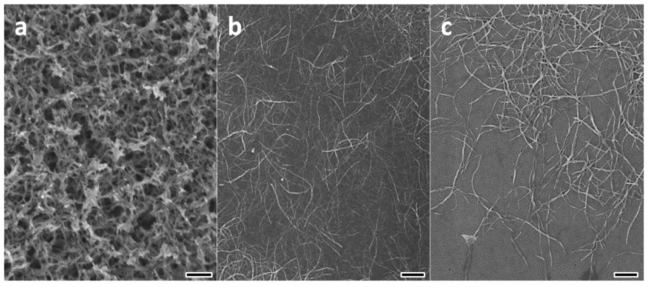

Figure 1. Scanning electron microscopy (SEM) images of (a) PANI synthesized via a standard rapidly mixed reaction procedure, (b) PANI synthesized via a rapidly mixed reaction but with the addition of aniline dimer (AD), and (c) PANI polymerized via a rapidly mixed reaction but with the addition of *p*-phenylenediamine (AP). Scale bar = 1 μm.

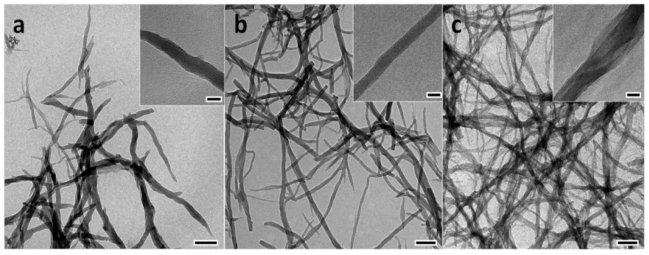

Figure 2. Transmission electron microscopy (TEM) images of (a) PANI synthesized via a standard rapidly mixed reaction without any additives, (b) PANI synthesized via a rapidly mixed reaction with the addition of aniline dimer (the AD sample), and (c) PANI polymerized via a rapidly mixed reaction with the addition of *p*-phenylenediamine (the AP sample). The insets offer a closer view of the individual nanofibers from the corresponding synthetic methods. Scale bar = 200 nm for the figures and 30 nm for the insets.

the samples were calculated from the sheet resistance and the thickness values.

III. RESULTS AND DISCUSSION

SEM images reveal a distinct difference between PANI nanofibers synthesized via a typical rapidly mixed reaction without any initiators and that with the addition of initiators such as aniline dimer or *p*-phenylenediamine, i.e., samples AD and AP, respectively (Figure 1). The conventional method without initiators yields an entangled network of PANI nanofibers with low aspect ratio (Figure 1a), whereas the same reaction with a small amount of either initiator generates much longer and less entangled nanofibers with much higher aspect ratios while maintaining the diameter of the nanofibers in the same range (Figure 1b,c). It is believed that initiators serve as homogeneous nucleation centers, which increase the reaction rate and lead to longer and less entangled 1-D nanostructured PANI.[30] The extra-long PANI nanofibers are highly dispersible in water (Figure 1b,c) and display better film-forming properties than conventional PANI nanofibers synthesized without an initiator (Figure 1a), which allows for easy preparation of high-quality films from aqueous dispersions.

Despite their apparently identical morphology as observed under SEM, the morphologies of the nanofibers from the AD and AP samples differ significantly upon closer inspection with TEM, as shown in Figure 2. The AD sample synthesized using aniline

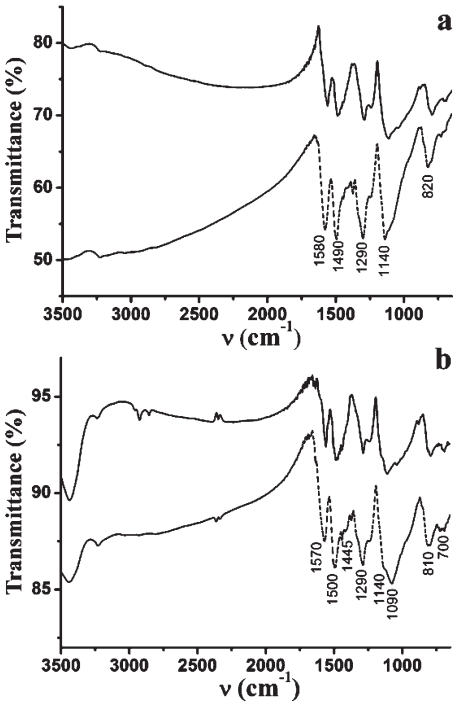

Figure 3. FT-IR spectra of PANI synthesized via a rapidly mixed reaction with the addition of aniline dimer, sample AD (a), and PANI polymerized via a rapidly mixed reaction with the addition of *p*-phenylenediamine, sample AP (b). Solid lines represent the spectra for the doped AD and AP samples, while the dashed lines represent the corresponding dedoped samples.

dimer exhibits a compact and smooth, rodlike morphology (Figure 2b) reminiscent of the nanofibers obtained without any additives (Figure 2a) despite the much higher aspect ratio. On the other hand, the TEM images of the sample AP reveal that the nanofibers are, in fact, comprised of smaller nanothreads that twist into bundles that each exhibits itself as an individual nanofiber (Figure 2c). This significant difference in morphology of the AP sample compared to the conventional and the AD PANI nanofibers is likely initiated at the atomic level which enables individual nanothreads to form coil-like structures. Since the synthetic conditions for samples AD and AP are identical except for the initiators incorporated, we can hypothesize that the structural differences in these additives initiate slightly different molecular structures of the polymer chains which subsequently results in the morphological variations in the final products. The para position in *p*-phenylenediamine is blocked, allowing this additive only to initiate the polymerization in the meta or ortho position. Such a mechanism initially favors the formation of cross-linked structures as opposed to the linear structures usually obtained due to para coupling. It is possible that these cross-linked structures dictate the formation of the coil-like nanofibers during the supramolecular assembly. Therefore, detailed structural analyses at the atomic level, i.e., solid-state NMR studies supported by other characterization techniques, are desirable in order to gain a better understanding as to whether and how these morphological differences are manifested by the molecular structures of the AD and AP samples.

FT-IR. The FT-IR spectra of the doped and dedoped samples of AD and AP are shown in parts a and b of Figure 3, respectively. These spectra share many common peaks and appear to exhibit

dx.doi.org/10.1021/ma102772t |*Macromolecules* 2011, 44, 2735–2742

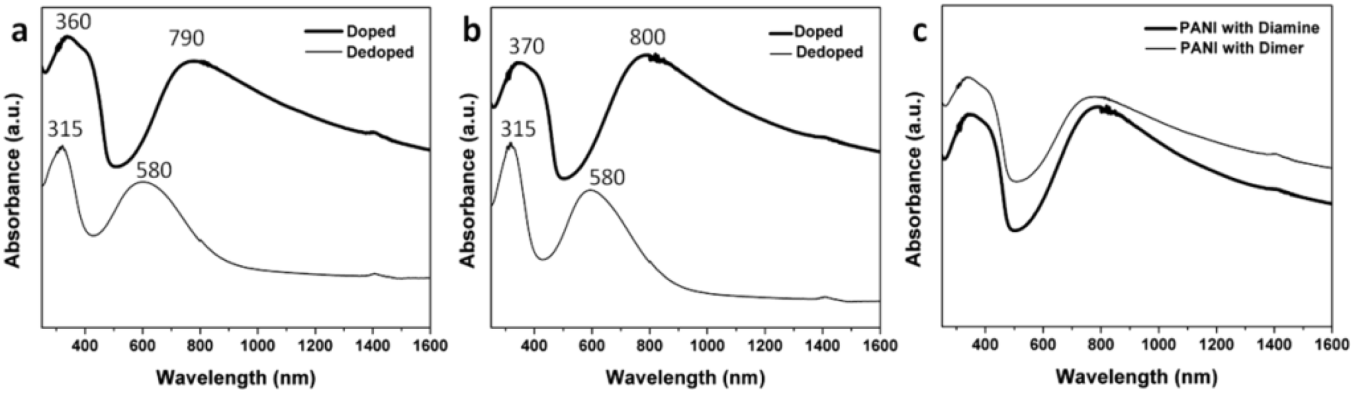

Figure 4. UV−vis−NIR spectra of PANI synthesized via a rapidly mixed reaction with the addition of aniline dimer, sample AD (a), and with the addition of *p*-phenylenediamine, sample AP (b). Spectra for the two doped samples are combined in (c) for comparison.

bands characteristic of "conventional" PANI.[1,32] This implies a prevalence of head-to-tail coupling, i.e., a relatively regular alternation of reduced and oxidized units. The bands at around 1580 and 1500 cm^{-1} can be attributed to C═C stretching in the quinoid and benzenoid rings, respectively. The shoulder at around 1445 cm^{-1}, which is clearly visible in the AP sample spectrum (Figure 3b), could be assigned to the phenazine-like or branched structures.[36] Because of the occupancy of the para position in the *p*-phenylenediamine molecule, cross-linking is likely favored at the beginning of the synthesis, which could be the underlying mechanism for the formation of coil-like nanofibers in the sample AP (see Figure 2b). The bands at around 1290 cm^{-1} originate from C−N stretching of the secondary aromatic amine. This band is more intense in the spectrum of the AD sample, which suggests the presence of a higher amount of amine nitrogen, i.e., benzenoid units. The shoulder (around 1240 cm^{-1}) is related to the protonated C−N group. The strong peaks that appear at ca. 1140 cm^{-1} are assigned to electronic bands that are usually considered to be a measure of the delocalization of electrons in the PANI structure.[1] This peak is more prominent in the AD sample which implies a better electron delocalization and consequently better conductivity. This could be partly a consequence of the more compact and homogeneous morphology as seen in Figure 2b. The bands at around 820 cm^{-1} originate from C−H out-of-plane bending in 1,4-disubstituted ring structures (para coupling), indicating the prevalence of the head-to-tail coupling during the polymerization.

UV−vis−NIR Spectroscopy. The UV−vis−NIR spectra of the AD and AP samples are shown in Figure 4 (a, sample AD; b, sample AP). Bold spectra are from the doped samples, while the thinner lines represent the corresponding dedoped samples. The UV−vis−NIR spectra of the doped samples show an absorption peak at around 370 nm, and a broad band at >800 nm with a tail that extends into the NIR region, which is an indication of the emeraldine salt oxidation state of PANI. The first absorption band arises from a $\pi-\pi^*$ electronic transition within the benzenoid segments. The second absorption band is related to the acid-doped state and polaron formation in the PANI structure. The spectra of the dedoped samples exhibit characteristic absorption for polyaniline in its emeraldine base state (Figure 4). The first band (315 nm) is assigned to $\pi-\pi^*$ excitation of the para-substituted benzenoid segment (−B−NH−B−NH), while the other (580 nm) is associated with the excitation of the quinoid segment (−N═Q═N−).

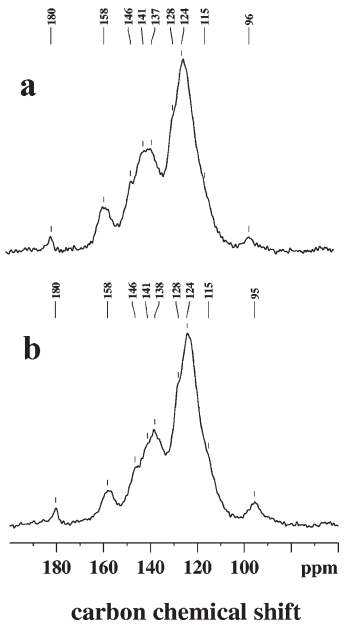

Figure 5. Solid-state ^{13}C CPMAS NMR spectra of (a) PANI synthesized via a rapidly mixed reaction with the addition of aniline dimer, sample AD, and (b) PANI polymerized via a rapidly mixed reaction with the addition of *p*-phenylenediamine, sample AP. Samples are in the dedoped emeraldine base oxidation state.

Scheme 2. Chemical Structure of PANI

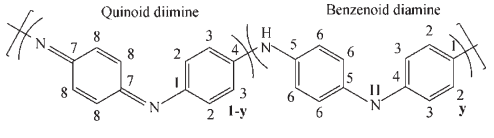

^{13}C CP MAS NMR Spectra. The solid-state ^{13}C CP spectra of the dedoped samples AD and AP are shown in parts a and b of Figure 5, respectively. The assignment of the resonance peaks in the ^{13}C CPMAS spectra shown in Figure 5 is based on the data obtained from "standard" chemically synthesized PANI.[34,37] The ^{13}C CP spectra of the AD and AP samples (Figure 5a,b) exhibit characteristic peaks (and intensities) similar to those seen in standard PANI spectra.[32]

The peak at 158 ppm is assigned to the nonprotonated imine quinoid carbon (C-7, see Scheme 2). The peak at 146 ppm is attributed to the nonprotonated carbon attached to the imine nitrogen C-1, consistent with the presence of quinoid rings. The peak for protonated quinoid carbon C-8 (≈137 ppm for "standard" chemically synthesized PANI, according to Kaplan et al.)[37] partly overlaps with the peak at ≈141 ppm due to the presence of the nonprotonated carbons (C-4 and C-5).[37] The peaks at 128 and 124 ppm are assigned to the protonated benzenoid carbons (C-2 and C-3).[37] The peak at 115 ppm is assigned to protonated benzenoid carbon (C-6) further away from the quinoid segment.[37] There are two low-intensity peaks at 96 and 180 ppm which are not characteristic of "conventional" chemically synthesized PANI. They are usually only detected in nanostructured PANIs.[6,35,38] The peak at 96 ppm is due to the presence of branching in the polymer structure.[35] The low-intensity signal at 180 ppm could be due to the presence of carbonyl groups on the six-membered rings. This was proposed previously in studies of similar materials.[39] As mentioned above, this carbonyl group could arise due to the presence of higher oxidation state of aniline, i.e., *N*-phenyl-1,4-benzoquinonediimine (PBQ), which can undergo a degradation reaction to produce quinoneimine end groups.[40] The overall shape for both spectra is similar to the spectrum of PANI and suggests the prevalence of regular head-to-tail sequencing characteristic of the presence of quinoid and benzenoid alternating segments and linear structures.

However, closer inspection reveals that the peak at 96 ppm is relatively more intense in the spectrum of the AP sample. This suggests that cross-linked structures are more favored initially, which is in line with the FT-IR spectra. These structures, although not present in a high amount, can serve as initial seeds from which twisted nanothreads structures are formed in the AP sample.

In general, it is difficult to discern slight differences in the structure solely from the ^{13}C spectra because of the lack of spectral resolution. Consequently, experiments using ^{15}N CP NMR were carried out because these spectra provide much better resolution. Usually ^{15}N CP MAS spectra of PANI exhibit two main peaks: amine (at ca. 65 ppm) and imine (at ca. 320 ppm). We have already applied ^{15}N CP NMR spectroscopy to describe the antioxidant properties of standard PANI and have correlated the results (based on the integration of peaks in the spectra) to XPS and elemental analysis.[32]

Since the resolution is much better, structural data obtained from such techniques can therefore shed light on the molecular structure−supramolecular assembly relationships of the PANI nanofibers synthesized with different initiators.

^{15}N NMR Spectra. The solid-state ^{15}N CP and DP MAS NMR spectra of the AD and AP samples are shown in Figure 6a−d.

CP MAS Spectra. The ^{15}N CP spectra of the samples AD and AP are shown in Figure 6a,c. The overall features of the spectra are different compared with the "conventional" PANI spectrum.[32] The first obvious difference is in the amine region. There are three distinct, partly overlapping peaks at 91, 70, and 38 ppm. These peaks are shifted downfield compared with the amine −NH peak (65 ppm), and the peak that corresponds to the $-NH_2$ end groups (ca. 30 ppm) which are usually observed in the spectrum of "conventional" PANI.[32] The two peaks at 70 and 90 ppm probably originate from the amine nitrogens in the segments that do have a different chemical environment or different conformations compared with "conventional" PANI.

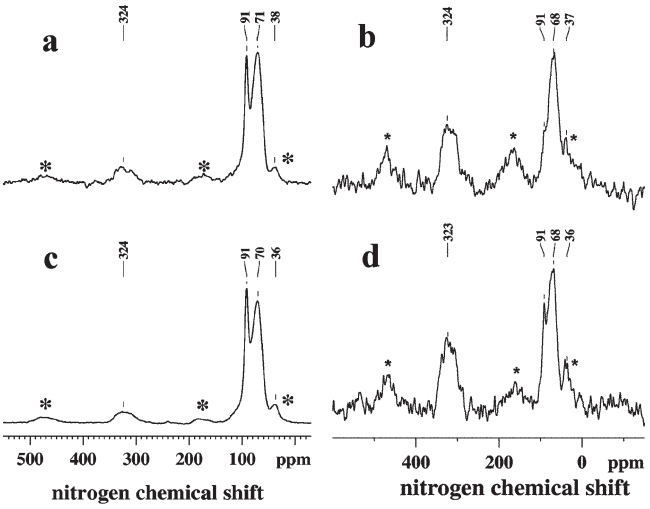

Figure 6. Solid-state ^{15}N CP (a, c) and DP (b, d) NMR spectra of (a, b) PANI synthesized via a rapidly mixed reaction with the addition of aniline dimer, sample AD, and (c, d) PANI polymerized via a rapidly mixed reaction with the addition of *p*-phenylenediamine, sample AP. The samples are all dedoped. The asterisks denote spinning sidebands.

The next significant feature is the *very low* intensity of the imine =N− peak at ∼320 ppm in both of the CP spectra (Figure 6a,c). Considering these results, the low intensity of the imine peak could be attributed to a *significantly underoxidized* material. Usually, determining the ratios of the amounts of different groups based on the integrated areas or peak intensities from CP/MAS NMR spectra is not straightforward. The enhanced signal intensity of the rare nucleus (carbon or nitrogen) depends on the kinetics of the transfer of magnetization from the abundant nucleus (usually ^1H). This transfer is mediated by the coupling between nuclei which occurs via a static dipolar interaction and has a $1/r^6$ dependence upon the internuclear distance r. The CP curve that describes a transfer of magnetization is complex since the initial signal buildup of the rare nucleus depends on the T_{IS} time, while the second, decaying part of the curve is due to the proton relaxation in the rotating frame, $T_1\rho^H$.[32,41,42] Thus, the signal as a function of time will pass through a maximum that is different for each group with a different degree of protonation or mobility. If rare nuclei are not protonated, i.e., directly bonded to a proton, they will cross-polarize more slowly than protonated ones. Also, the more rigid groups will have faster signal buildup during the transfer because of lesser averaging of dipolar interactions due to molecular motion. In order to get quantitative data, the different affinity of various groups toward the polarization enhancement must be taken into account.[32,41,42] To get the corrected imine/amine ratio, variable contact time experiments were performed. The data are summarized in Table 1. The observation of significantly longer T_{IS} (T_{NH}) values for the imine groups compared to those of the amine groups is attributed to nonprotonation of the former. The corrected integrated areas (see eq 1), obtained from the spectra recorded at a contact time of 1.5 ms, are listed in Table 1.

$$C = \frac{I\left(1 - \frac{T_{IS}}{T_{1\rho}^H}\right)}{\exp\left(-\frac{t_{cp}}{T_{1\rho}^H}\right) - \exp\left(-\frac{t_{cp}}{T_{IS}}\right)} \quad (1)$$

Table 1. Data from ^{15}N Variable Contact Time, Direct Polarization (DP), and Cross-Polarization (CP) Experiments for the Samples AD and AP

	relaxation constants				integrated area (normalized)			
sample	$T_{1\rho H}$ (ms)	T_{NH} (μs)	T_{1H}(N) (ms)	T_{1H}(H) (ms)	DP (%)	ratio	CP (corr) (%)	ratio
AD								
imine	3.0	2500	150	240	45	0.82	22	0.28
amine	3.4	55	250		55		78	
AP								
imine	5.5	3000	500	480	50	1.0	23	0.30
amine	5.1	70	490		50		77	

The integrated intensity for the imine peak includes the peak at 324 ppm. The integrated intensities obtained from deconvolution have an error of ~10%. The imine-to-amine ratio (the ratio of the corrected integrated areas for peaks at around 70 and 90 (A^{NH}) and 320 ppm (A^{N}) and its related sidebands) is ca. $A^{N}/A^{NH} = 0.3$ (Table 1).

However, the FT-IR, UV−vis, and ^{13}C CP spectra suggest the prevalence of head-to-tail coupling similar to standard PANI and a significantly higher value for the imine/amine ratio, probably closer to 1.0.

This is something that we have already noticed for other nanostructured material obtained by oxidative polymerization of aniline.[4,6] Therefore, we want to explore these discrepancies here.

Apart from the CP parameters, another critical factor for quantification is the T_{1H} relaxation time that determines the recycle delay of the experiment. Not taking this parameter into account could lead to spectra with distorted intensities. The T_{1H} relaxation times for hydrogen are obtained by means of two different experimental approaches: proton (T_{1H}(H)) and nitrogen (T_{1H}(N)) detection. In cases with proton detection, the average T_{1H}(H) time was around 240 ms for AD and 480 ms for AP (Table 1). These are average values obtained from one broad peak since the lack of resolution in the ^{1}H spectra did not allow resolution of individual peaks for different structural units, such as imine or amine. On the other hand, the experiments with ^{15}N detection offer much better resolution, and the relaxation times can be obtained for different structures. Therefore, the relaxation times for imine and amine groups can be acquired separately. Thus, we obtained T_{1H}(N) times of ca. 500 ms in the AP sample and 150 and 250 ms in the AD sample for imine and amine groups, respectively (Table 1). Knowing that 3−5 T_1 is sufficient for a recycle delay to get quantitative spectra, we used 2−3 s. As we took into consideration all of the relevant parameters during the CP experiment, the only thing that could have affected quantification is the remoteness of the hydrogen nuclei from the nitrogen. This means that the imine/amine ratio obtained from CP experiments on nanostructured PANI could be significantly undervalued.

For this reason, we carried out DP experiments that are independent of the presence of hydrogen, as shown in Figures 6b and 6d for samples AD and AP, respectively. Although an experimental time could be very long, these kind of experiments do not suffer from the usual quantification problems often seen in CP.[38]

There are apparent differences between the spectral characteristics of DP and CP spectra. Most striking is a much larger contribution of imine groups, since the peaks at 320 ppm are much more intense compared to their CP counterparts. The imine/amine ratios for the samples A and B were 0.82 and 1.0, respectively (see Table 1). These values are different to the data obtained using the CP technique (Table 1) and closer to the ones that can be deduced from FT-IR, UV−vis, and ^{13}C CP experiments. A possible reason for this difference could be a difference in the proton environments of the N atoms in the different kinds of material (e.g., protons are more remote from the N atoms in the nanotube material) or a difference in the proton dynamics (e.g., fast exchange of hydrogen-bonded protons between =O and =N and H−N in the self-assembled nanotubes[4,6]). However, the nucleus of interest (^{15}N here) with intramolecular protons within two or three bonds should usually have signal intensities in line with atomic ratios. In other words, imine nitrogens must be four or more bonds away from protons to be undetected.[42] A further possible explanation can be that the proton spin bath consists of small proton domains which are somehow disconnected from the rest of the spin bath. Some of the imine nitrogens could be located close to these protons.

Alternatively, polarization transfer in standard PANI might be facilitated because this material exhibits a featureless granular morphology in which grains are packed together very closely and randomly distributed.

This implies that special care should be taken when the CP solid-state NMR technique is used for PANI nanostructured materials. In other words, using only CP to quantify different groups could be problematic. This is not the case for conventional PANI where the imine/amine ratio can be determined relatively accurately from ^{15}N CP MAS spectra.[32,43]

Structural Characteristics of Ultralong Nanofibers. Polyaniline nanofibers synthesized with different initiators do not vary significantly in molecular chain structure.[30,31] The slight differences observed in molecular structure likely arises from the different oligomers formed at the initial stage of polymerization. However, this small divergence in oligomer structure dictates the assembly of the polymer chains and dramatically affects the morphology, despite its minor influence on their physical properties.

The slightly cross-linked structures of the AP sample are evident from the FT-IR and ^{13}C CP NMR spectra due to ortho coupling as mentioned earlier. *p*-Phenylenediamine has a lower oxidation potential than aniline and hence is more reactive and oxidizes first.[30] Since the para position is occupied, the *p*-phenylenediamine molecules couple with each other along with some aniline molecules at the ortho position and form branched structures as a comparable study has proposed.[44] The effects of mobility can be observed from the relaxation data summarized in Table 1. The nanofibers obtained with *p*-phenylenediamine (AP)

are less mobile and have longer T_{1H} and $T_{1\rho H}$ relaxation times. This is likely due to the fact that the individual nanothreads are twisted into bundles that exhibit as individual nanofibers, and therefore their chain mobility is constrained (tightly packed structure). The underlying reason can again be attributed to the intermolecular cyclization of the initiator molecules occurring at the early stage of the synthesis as the para position of *p*-phenylenediamine is occupied.[45]

Previous studies have suggested that the cyclization reaction leads to the formation of phenazine-like rings that are planar and flat; hence, they tend to aggregate through $\pi-\pi$ stacking and van der Waals interactions.[36] This mechanism allows for the phenazine-like units to form a semiordered core similar to the aniline oligomer core when aniline dimer is used as the initiator.[36] Our previous study has indeed shown that low molecular weight oligomers can form crystalline structures that are much more ordered than polyaniline nanofibers.[46] The reaction then proceeds with the para coupling mechanism due to the high acidity of the reaction environment. The polymer chain is likely to self-assemble into the nanofibrillar morphology as the PANI chains bind to the flat core in a spiral motion, guided and stabilized by hydrogen bonding and ionic interactions, and extend along the fiber long axis. A similar mechanism has previously been proposed in studies on PANI nanotubes.[36] This mechanism has likely led to the formation of nanothreads that eventually twist into long nanofibers. UV−vis−NIR data further support this proposed mechanism. The asymmetric broad peak around 800 nm that extends into the NIR region in doped PANI spectra is indicative of polaron delocalization.[47−49] Larger broadening and tailing effects are associated with the straightening of the polymer chains, which can be used as a measure of their linearity.[47−49] Figure 4c combines the doped spectra for the AD and the AP samples. The AD sample has a broader peak around 800 nm and also exhibits a slightly stronger tailing effect. This suggests that the polymer chain is slightly more stretched/straighter in the AD sample than that in the AP sample. Such observations agree with our proposed mechanism as the polymer chain conformation is likely to be less extended in the AP sample due to the spiral chain packing mechanism that eventually leads to nanofibers comprised of bundles of twisted nanothreads as observed in TEM. The minor difference in molecular structures of the PANI nanofibers synthesized with aniline dimer and *p*-phenylenediamine also have an effect on the electrical properties of the final polymer. The AD PANI possesses an electrical conductivity of 3.0 S cm^{-1}, while the AP sample has a conductivity of 1.7 S cm^{-1}. The conductivity for both samples are of the same order of magnitude, but the slightly lower conductivity of the AP sample could be attributed to the small amount of the cross-linked, insulating core formed during the early stage of the polymerization that serves as a nonconjugated defect in the polymer chain that subsequently hinders carrier transport. The less extended chain conformation of the PANI nanofibers synthesized with the *p*-phenylenediamine could have also contributed to the slightly lower conductivity compared to its counterpart synthesized with aniline dimer as the initiator.

Recently, the morphology and the formation of PANI nanofibers were investigated in light of nucleation theory.[50] It was suggested that heterogeneous nucleation during the formation of PANI nanofibers favors agglomerated structures while homogeneous nucleation promotes more nanofibrillar morphologies.[50]

We can see how our findings further support this theory. The additives rapidly form growth centers for polymerization since they have a lower oxidation potential than aniline.[30] Therefore, the nucleation should be initiated simultaneously throughout the solution (homogeneous nucleation), and the diffusion to heterogeneous nucleation sites should be limited.[45] We can hypothesize that the different morphologies of nanofibers synthesized here are due to homogeneous nucleation. Since the structure of the nucleation sites depends on the structure of the additives, the initially formed nucleation sites will determine the morphological characteristics of later products. For example, since the para-position in *p*-phenylenediamine is hindered, the polymerization will be initiated in the meta or ortho position, which favors the formation of cross-linked structures that further dictate the assembly of the coil-like nanofibers.

The differences in molecular structure and assembly mechanism could also explain why the choice of initiator is such a crucial factor in PANI derivative nanofiber formation. Unlike PANI, the nanofibrillar morphology is not intrinsic to PANI derivatives; hence, the presence of an initiator is essential in such reactions if nanofibers or other 1-D nanostructures are desired.[19] It is likely that only one of the two reaction mechanisms is suitable for a particular PANI derivative to form nanofibers, i.e., using aniline dimer to form a semirigid core that can dictate the nanofiber growth versus allowing the stacked planar, cross-linked segments formed from the oxidation of *p*-phenylenediamine to cause the polymer chains to assemble in a spiral motion. Therefore, our study also explains why the choice of initiator plays a central role in the supramolecular assembly of PANI derivatives.

IV. CONCLUDING REMARKS

The addition of a small amount of an initiator, *p*-aminodiphenylamine (dimer) or *p*-phenylenediamine (diamine), leads to higher aspect ratio PANI nanofibers that are less entangled compared to PANI nanofibers synthesized without any initiators. Careful TEM analysis reveals a striking difference in morphology between the PANI nanofibers synthesized with the aniline dimer as the initiator and that with *p*-phenylenediamine, which have been considered identical in morphology in previous studies. FT-IR, ^{13}C cross-polarization, ^{15}N direct polarization solid-state NMR, and UV−vis spectroscopy confirm that a regular head-to-tail coupled polyaniline structure prevails in both types of nanofibers, indicating that the nanofibers synthesized with different initiators do not differ significantly in atomic structure. However, the minor divergence in molecular structure, likely due to the differing oligomer structures created as a result of the different initiators used, has a considerable effect on the supramolecular assembly. On the other hand, ^{15}N cross-polarization solid-state NMR has shown significantly different spectral characteristics from those expected for a regular PANI structure. The imine/amine ratio obtained from integrated intensities in $^{1}H-^{15}N$ cross-polarization experiments is 0.3 for both nanofibers. Nevertheless, from the ^{15}N DP experiments the imine/amine ratios are closer to 1.0, indicating head-to-tail coupling and a standard polyaniline structure. The reason for this is probably the greater distance of the imine nitrogens from the hydrogens as indicated in relaxation experiments. The other explanation could be the heterogeneous nature of the proton spin bath which eventually causes a preferential polarization transfer. The relationship between molecular structure and assembly mechanism also sheds light on why the choice of initiator is a crucial factor in PANI derivative nanofiber formation, an observation that could not be explained previously. It is likely that only one of the

mechanisms that arise from the two different initiators is suitable for a certain PANI derivative to form nanofibers. We believe that homogeneous nucleation affects the morphological characteristics of nanofibers obtained in the presence of additives. Exquisite control of supramolecular morphologies should be possible for a large number of conducting polymers by introducing a suitable molecule as the initiator.

AUTHOR INFORMATION

Corresponding Author

*E-mail: z.zujovic@auckland.ac.nz.

ACKNOWLEDGMENT

The authors thank Dr. Henry D. Tran for performing some preliminary experiments and for helpful discussions. Support for this research has been provided by the UCLA based Focused Center Research Program in Functional Engineered NanoArchetectonics (R.B.K.) and a National Science Foundation—Graduate Research Fellowship (Y.W.).

REFERENCES

(1) *Handbook of Conducting Polymers*, 3rd ed.; Skotheim, T. A., Elsenbaumer, R. L., Reynolds, J. R., Eds.; Marcel Dekker: New York, 2007.
(2) Stejskal, J.; Sapurina, I.; Trchová, M. *Prog. Polym. Sci.* **2010**, *35*, 1420–1481.
(3) Laslau, C.; Zujovic, Z.; Travas-Sejdic, J. *Prog. Polym. Sci.* **2010**, *35*, 1403–1419.
(4) Zujovic, Z. D.; Laslau, C.; Bowmaker, G. A.; Kilmartin, P. A.; Webber, A. L.; Brown, S. P.; Travas-Sejdic, J. *Macromolecules* **2010**, *43*, 662–670.
(5) Zujovic, Z. D.; Laslau, C.; Travas-Sejdic, J. *Chem.—Asian J.* **2011**, *6*, 791.
(6) Zujovic, Z. D.; Zhang, L.; Bowmaker, G. A.; Kilmartin, P. A.; Travas-Sejdic, J. *Macromolecules* **2008**, *41*, 3125–3135.
(7) Lim, J. A.; Liu, F.; Ferdous, S.; Muthukumar, M.; Briseno, A. L. *Mater. Today* **2010**, *13*, 14–24.
(8) Ciric-Marjanovic, G. In *Nanostructured Conductive Polymers*; Eftekhari, A., Ed.; Wiley: London, 2010; Chapter 2, p 19.
(9) Ciric-Marjanovic, G.; Dondur, V.; Milojevic, M.; Mojovic, M.; Mentus, S.; Radulovic, A.; Vukovic, Z.; Stejskal, J. *Langmuir* **2009**, *25*, 3122–3131.
(10) Ciric-Marjanovic, G.; Dragicevic, L.; Milojevic, M.; Mojovic, M.; Mentus, S.; Dojcinovic, B.; Marjanovic, B.; Stejskal, J. *J. Phys. Chem. B* **2009**, *113*, 7116–7127.
(11) Zhang, D.; Wang, Y. *Mater. Sci. Eng., B* **2006**, *134*, 9–19.
(12) Jang, J. *Adv. Polym. Sci.* **2006**, *199*, 189–259.
(13) Huang, J.; Kaner, R. B. *Chem. Commun.* **2006**, 367–376.
(14) Wu, C. G.; Bein, T. *Science* **1994**, *264*, 1757–1759.
(15) Martin, C. R. *Acc. Chem. Res.* **1995**, *28*, 61–68.
(16) Wei, Z.; Zhang, Z.; Wan, M. *Langmuir* **2002**, *18*, 917–921.
(17) Qiu, H.; Wan, M.; Matthews, B.; Dai, L. *Macromolecules* **2001**, *34*, 675–677.
(18) Zhang, Z.; Wan, M.; Wei, Y. *Adv. Funct. Mater.* **2006**, *16*, 1100–1104.
(19) Anilkumar, P.; Jayakannan, M. *Macromolecules* **2007**, *40*, 7311–7319.
(20) Zhang, X.; Goux Warren, J.; Manohar Sanjeev, K. *J. Am. Chem. Soc.* **2004**, *126*, 4502–4503.
(21) Niu, Z.; Bruckman, M. A.; Li, S.; Lee, L. A.; Lee, B.; Pingali, S. V.; Thiyagarajan, P.; Wang, Q. *Langmuir* **2007**, *23*, 6719–6724.
(22) Huang, J.; Virji, S.; Weiller, B. H.; Kaner, R. B. *J. Am. Chem. Soc.* **2003**, *125*, 314–315.
(23) Huang, J.; Kaner, R. B. *J. Am. Chem. Soc.* **2004**, *126*, 851–855.
(24) Huang, J.; Kaner Richard, B. *Angew. Chem., Int. Ed.* **2004**, *43*, 5817–5821.
(25) Chiou, N.-R.; Epstein, A. J. *Synth. Met.* **2005**, *153*, 69–72.
(26) Chiou, N.-R.; Epstein, A. J. *Adv. Mater.* **2005**, *17*, 1679–1683.
(27) Jing, X.; Wang, Y.; Wu, D.; Qiang, J. *Ultrason. Sonochem.* **2007**, *14*, 75–80.
(28) Pillalamarri, S. K.; Blum, F. D.; Tokuhiro, A. T.; Story, J. G.; Bertino, M. F. *Chem. Mater.* **2005**, *17*, 227–229.
(29) Huang, J.; Kaner, R. B. *Angew. Chem., Int. Ed.* **2004**, *43*, 5817–5821.
(30) Tran Henry, D.; Wang, Y.; D'Arcy Julio, M.; Kaner Richard, B. *ACS Nano* **2008**, *2*, 1841–1848.
(31) Tran, H. D.; Norris, I.; D'Arcy, J. M.; Tsang, H.; Wang, Y.; Mattes, B. R.; Kaner, R. B. *Macromolecules* **2008**, *41*, 7405–7410.
(32) Zujovic, Z. D.; Gizdavic-Nikolaidis, M. R.; Kilmartin, P. A.; Idriss, H.; Senanayake, S. D.; Bowmaker, G. A. *Polymer* **2006**, *47*, 1166–1171.
(33) Zhang, L.; Peng, H.; Zujovic, Z. D.; Kilmartin, P. A.; Travas-Sejdic, J. *Macromol. Chem. Phys.* **2007**, *208*, 1210–1217.
(34) Zujovic, Z. D.; Bowmaker, G. A.; Tran, H. D.; Kaner, R. B. *Synth. Met.* **2009**, *159*, 710–714.
(35) Zujovic, Z. D.; Laslau, C.; Bowmaker, G. A.; Kilmartin, P. A.; Webber, A. L.; Brown, S. P.; Travas-Sejdic, J. *Macromolecules* **2009**, *43*, 662–670.
(36) Konyushenko, E. N.; Stejskal, J.; Sedenkova, I.; Trchova, M.; Sapurina, I.; Cieslar, M.; Prokes, J. *Polym. Int.* **2006**, *55*, 31–39.
(37) Kaplan, S.; Conwell, E. M.; Richter, A. F.; MacDiarmid, A. G. *Synth. Met.* **1989**, *29*, E235–E242.
(38) Hopkins, A. R.; Lipeles, R. A.; Hwang, S.-J. *Synth. Met.* **2008**, *158*, 594–601.
(39) Venancio, E. C.; Wang, P.-C.; MacDiarmid, A. G. *Synth. Met.* **2006**, *156*, 357–369.
(40) Gospodinova, N.; Mokreva, P.; Terlemezyan, L. *Polymer* **1994**, *35*, 3102–3106.
(41) Pines, A.; Gibby, M. G.; Waugh, J. S. *J. Chem. Phys.* **1973**, *59*, 569–590.
(42) Alemany, L. B.; Grant, D. M.; Pugmire, R. J.; Alger, T. D.; Zilm, K. W. *J. Am. Chem. Soc.* **1983**, *105*, 2142–2147.
(43) Mathew, R.; Yang, D.; Mattes, B. R.; Espe, M. P. *Macromolecules* **2002**, *35*, 7575–7581.
(44) Cotarelo, M. A.; Huerta, F.; Quijada, C.; Mallavia, R.; Vazquez, J. L. *J. Electrochem. Soc.* **2006**, *153*, D114–D122.
(45) Gizdavic-Nikolaidis, M. R.; Stanisavljev, D. R.; Easteal, A. J.; Zujovic, Z. D. *J. Phys. Chem. C* **2010**, *114*, 18790–18796.
(46) Wang, Y.; Tran, H. D.; Liao, L.; Duan, X.; Kaner, R. B. *J. Am. Chem. Soc.* **2010**, *132*, 10365–10373.
(47) MacDiarmid, A. G.; Epstein, A. J. *Synth. Met.* **1994**, *65*, 103–116.
(48) Rannou, P.; Gawlicka, A.; Berner, D.; Pron, A.; Nechtschein, M.; Djurado, D. *Macromolecules* **1998**, *31*, 3007–3015.
(49) Xia, Y.; Wiesinger, J. M.; MacDiarmid, A. G.; Epstein, A. J. *Chem. Mater.* **1995**, *7*, 443–445.
(50) Li, D.; Kaner, R. B. *J. Am. Chem. Soc.* **2006**, *128*, 968–975.